

FINITE ELEMENT ANALYSIS FOR STRUCTURAL HEALTH MONITORING OF HELICOPTER AIRFRAMES

Francisco Javier San Millán*, Malte Frövel*, Roberto González*

*Instituto Nacional de Técnica Aeroespacial (INTA), Materials and Structures Department
Carretera de Ajalvir km 4. 28850 Torrejón de Ardoz, Madrid (Spain)
sanmillan@inta.es, frovelm@inta.es, gonzalezar@inta.es

Key words: Structural Health Monitoring (SHM), FEA (Finite Element Analysis), ANN (Artificial Neural Network), Stress Intensity Factor (SIF).

Summary: *ASTYANAX is a Research project promoted by the EDA (European Defence Agency), focused on the development of reliable methodologies for Structural Health Monitoring (SHM) of rotary and fixed-wing platforms. Two types of damages, quite common in helicopter and aircraft airframes, are studied: local plastifications caused by overloads such as hard landings, and cracks growing in fatigue. Within the project, SHM systems with diagnostic and prognostic capabilities are designed based in Artificial Neural Networks (ANN) algorithms, while Finite Element Analysis (FEA) of the damaged and undamaged airframe structure, are used to generate the simulated experience required for ANN training. In the paper the FEA approach used for the fatigue crack SHM system is explained, that includes parametric FEM versions considering multiple crack configurations. Validation of the FEA, and the SHM system itself, will be made with the sensor readings during the fatigue tests, that will be made to a full scale metallic helicopter equipped with a sensor network of PZTs and optical sensors.*

1 INTRODUCTION

ASTYANAX is a Research project promoted by the EDA (European Defence Agency), focused on the development of reliable methodologies for Structural Health Monitoring (SHM) of rotary and fixed-wing platforms. ASTAYNAX is the follow-on of preceding EDA project HECTOR [1][2], and the objective for the Technology readiness level (TRL) of the developed SHM systems is between 5 and 6, while in HECTOR project TRL was 3.

The project focuses in 2 types of damages relatively common in helicopter airframes: local plastifications in stressed areas caused by hard landings, and cracks originated in rivet holes that grow in fatigue during the operational life of the vehicle.

Within the project a complete set of activities related to SHM methodologies are carried out: study of state of the art of SHM components (sensors for instance), development of damage detection algorithms, Finite Element Analysis (FEA) of the damaged and undamaged structure, sensor network technologies, SHM systems reliability, Tests, etc. A Cost-Benefit Analysis of the proposed SHM systems will be made as well, quantifying the benefit of Condition Based Maintenance approach on an aerial platform.

Demonstrations are made to a full scale helicopter: the Mi 8/17 Hip. Two kind of tests are

performed, the first one are drop tests from increasing height (already performed during 2014), made to the whole helicopter (weight 12 Tons) with the aim of identifying the onset of local plastifications.



Figure 1: Mi 8/17 Hip helicopter



Figure 2: Drop Test execution (April 2014)

The other main tests carried out are fatigue tests of the helicopter tail boom (TB). An initial notch will be performed to the TB, and during the tests the crack size will be monitored. Additionally, the TB will be equipped with a sensor network. The reading of these sensors (mainly mechanical strains) will be the inputs of an SHM system designed within ASTYANAX with diagnostic and prognostic capabilities. This SHM system has been designed by using Artificial Neural Networks (ANN) algorithms.

In the paper the FEA approach used for the TB and the fatigue crack process is explained in detail. The FEA has a double aim: first to simulate the fatigue tests and to determine relevant test features such as the adequate size of the initial notch, the critical crack length, the crack growth rate, and the sensitivity of strain sensor readings to crack length.

On the other hand, parametric versions of the TB FEM considering multiple crack positions or configurations, are used to generate the training database of the SHM system that will be verified at the fatigue Tests. ANN algorithms, the heart of the SHM system, requires a high number of cases in the order of thousands or more, for a proper training.

FEA accuracy is, therefore, very important for an adequate design of the SHM systems. The strategies followed for FEM parameterization and automation, and for derivation of strain and Stress Intensity Factor (SIF) results are explained in this paper.

2 HELICOPTER GLOBAL FEM

The helicopter global FEM was prepared by AFIT (Instytut Techniczny Wojsk Lotniczych from Poland) using the solver MSC.Nastran [3][4][5] and the Pre/post Patran [6][7][8]. It consists of three primary parts: the cockpit, the fuselage (assembly of front, mid, rear fuselage, fuel tank, and landing gear), and the TB.

The analyses made with the global FEM include static load cases, dynamic simulations (multibody analysis) for hard landing loads, and fatigue and crack propagation analyses. In Figure 3 and Figure 4 some images of the Mi 8/17 Hip global FEM are shown.

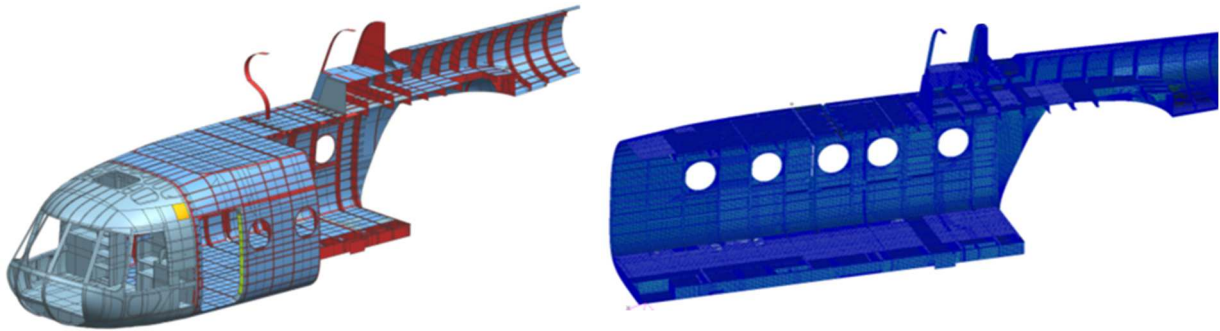


Figure 3: General view of Mi 8/17 global FEM (© AFIT)

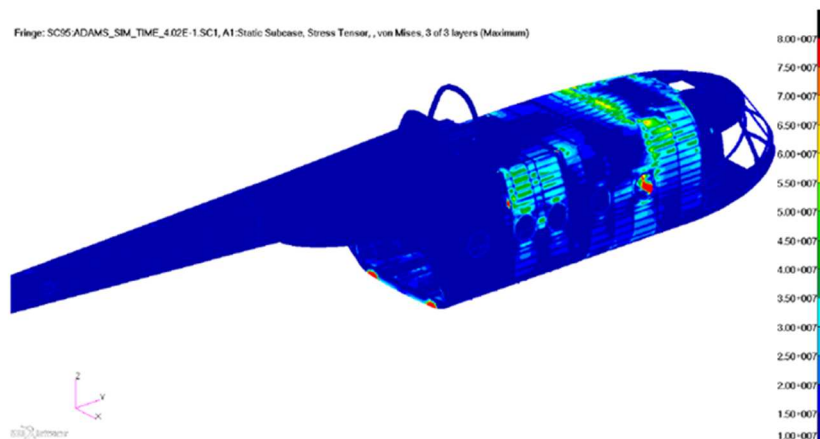


Figure 4: Multibody simulation for hard landing (© AFIT)

2.1 Tail boom (TB) global FEM

The Mi 8/17 TB is an aluminium stiffened structure (5.4 m long), comprising:

- Skin.
- Stringers (L shape).
- Frames with cuts allowing stringers crossing.
- Rivets connecting skin to stringers, skin to frames, and stringer to frames.

In Figure 5 an internal view of the TB is shown, while in Figure 6 a global view of the TB global FEM is shown.



Figure 5: TB internal view

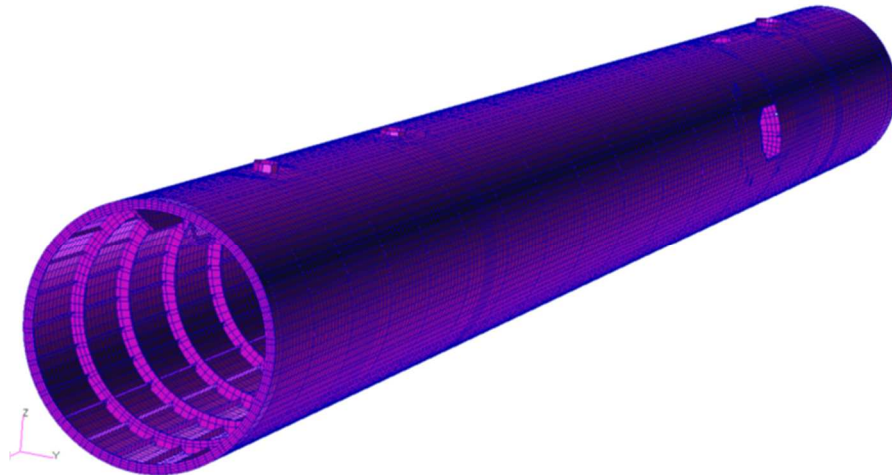


Figure 6: TB global FEM (© AFIT)

3 TB FATIGUE TESTS

The TB Fatigue Tests will be carried out during this year 2015. The TB is a 5.4 m long structure, and will be mounted in a rig, and tested to fatigue loads representative of in service tail-rotor forces: $F_Y = 20$ KN, $R = 0.1$ (TBC). In Figure 7 a scheme of the Fatigue Tests is shown. As above explained, an initial notch will be made to the TB, and during the tests the crack size will be monitored.

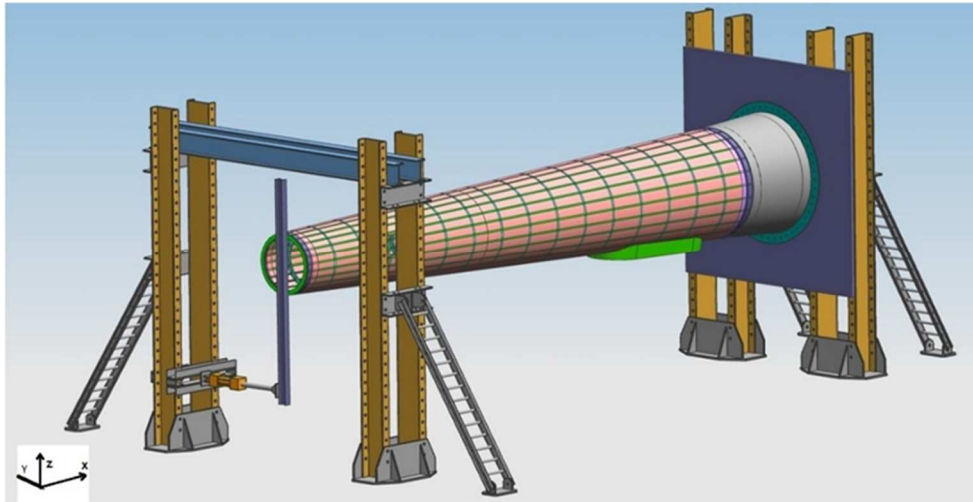


Figure 7: Fatigue Tests scheme

3.1 Initial notch and sensor installation

An analysis of the global TB FEM, with a load case proportional to the Fatigue Test load was done, and the zone with highest stresses was, as expected, close to the TB support (see Figure 8).

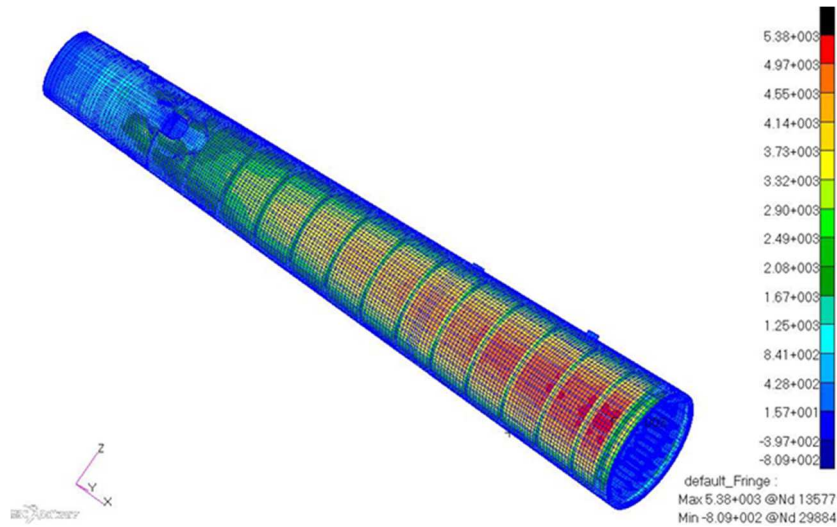


Figure 8: Maximum principal stress (Pa)

Based in these results, the “sensorized” part of the TB is selected between frames 2 and 3, and covering 6 bays: between stringers 5 and 11. The initial notch will be performed in this part of the TB as well. In Figure 9, this part of the TB is identified.

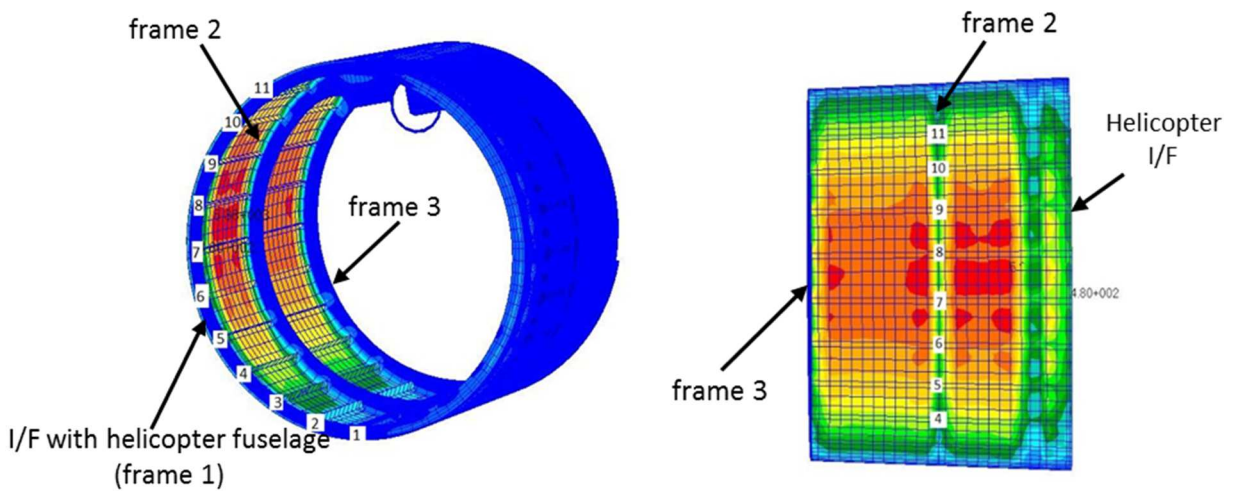


Figure 9: TB FEM, stress plot detail

The sensors used for the TB will be, among others, optical Fibre Bragg Grating sensors (FBGS) bonded to the stringers measuring longitudinal strain. As above explained, the readings of the different sensor are actually the inputs of the SHM system that has been designed within ASTYANAX, and that has diagnostic capabilities: crack detection, crack localization, and crack quantification, and prognostic capabilities: estimation of the TB residual life.

This “sensorized” part of the TB is analysed by means of a detailed local FEM that it is carefully explained in the next section.

4 LOCAL TB FEM

The global - local approach is used for the FEA. The global FEM passes over local details not affecting its overall behaviour, such as cut-outs, joints, etc. Such details are incorporated into a local FEM that includes crack modelling as well.

In Figure 10 a general view of the local TB FEM is shown, it was prepared by INTA using the solver MSC.Nastran and the Pre/post Patran. In Figure 11 a detail of the frames and stiffener crossing can be seen.

2D shell elements (CQUAD4 and CTRIA3 in Nastran terminology) are used mainly for the local FEM, while rivets are modelled by means of CFAST connectors [8]. Connectors are a useful tool to join non-congruent meshes, and can be used to simulate mechanical elements such as fasteners or rivets, incorporating into the FEM the axial and shear stiffness of these elements.

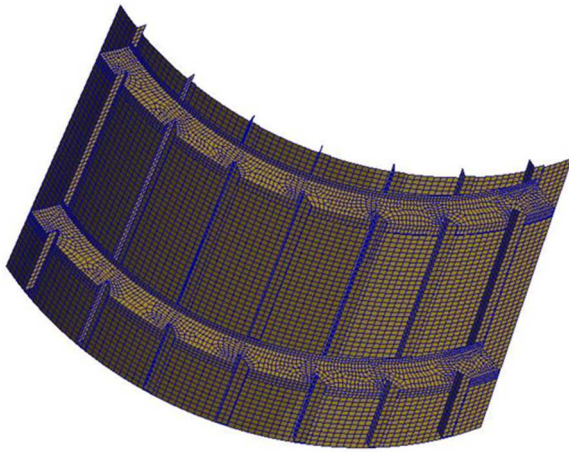


Figure 10: Local FEM (un-cracked configuration)

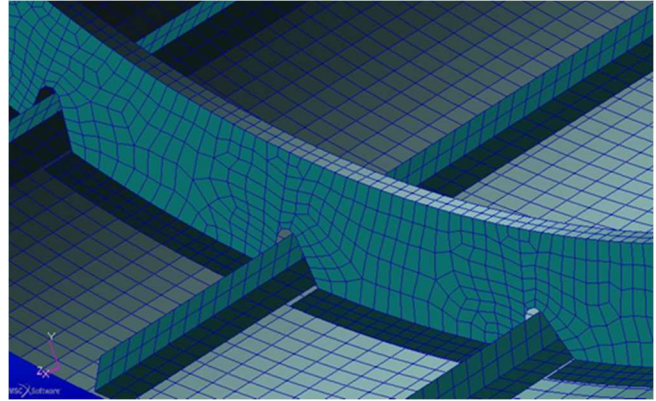


Figure 11: Detail of frames and stringers crossing

The local FEM is used for two purposes. In the one hand, to simulate the TB fatigue test providing support to determine important features of the tests: an adequate size of the initial notch, the critical crack length, the crack growth rate, and the sensitivity of the strain read by the sensors to crack length.

On the other hand, parametric versions of the local FEM considering multiple crack configurations, generate the training database of the SHM system. This SHM system has been designed by using ANN algorithms. An un-cracked local FEM is prepared as well, whose results are a reference for the ANN algorithms.

The parameters for the “family” of cracked local FEMs are crack position, crack length, and crack angle. From the local FEMs, SIF and strain results are derived. In Figure 12, the overall scheme of the FEA carried out for the fatigue crack SHM system, and the simulation of fatigue Tests within ASTYANAX is shown.

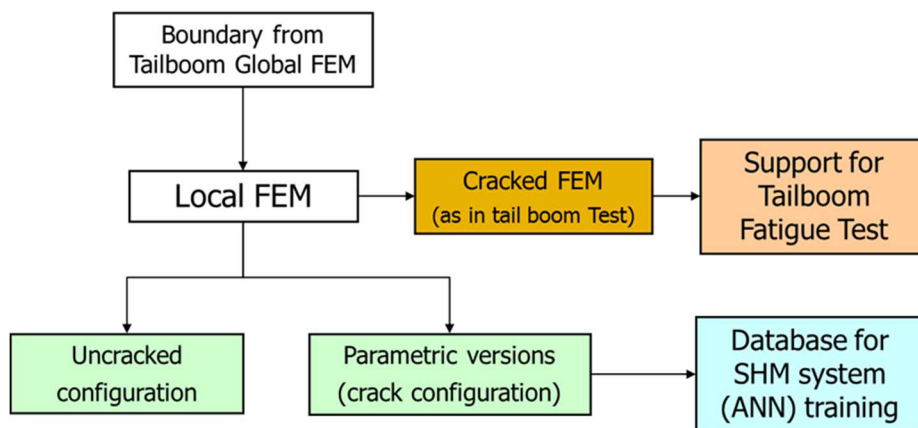


Figure 12: FEA scheme

4.1 Global-local FEA

Global-local FEA require some boundary of interface conditions for the local FEM. Several options are available [9]:

- **Multi-scale analysis**, with two possibilities: displacement and force Approaches.

Results from global FEA, displacements plus rotations in the first approach or internal forces plus moments in the second one, are used as boundary conditions in the local FEM edges. This method is very effective and if done properly is quite accurate.

- **Integrated analysis:** It means that the local FEM is actually inserted within the global FEM. Different approaches are available for the integrated analyses: mesh refinement, interface elements (MPCs for instance), and glued constraint.
- **SuperElements (SE):** SE is a reduction of stiffness and mass matrices of the global FEM into the boundary nodes of the local FEM. Several approaches are available as the Guyan reduction (static condensation), and for dynamic analysis the Craig-Bampton fixed interface method and the MacNeal's approach. More details can be found in [5].

For the ASTYANAX TB FEM the multi-scale analysis with displacement approach, has been used because its simplicity and because it is almost automatic inside the Pre/post Patran. In Figure 13, a partial view of the local TB FEM loaded with the boundary displacements plus rotations from global FEA can be seen.

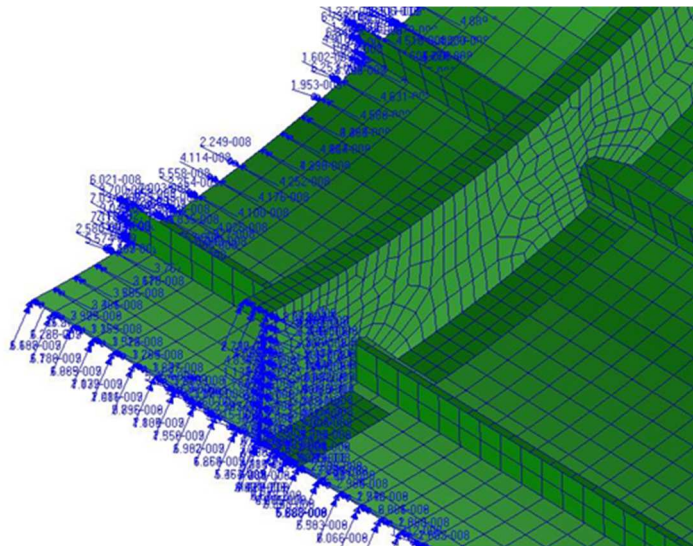


Figure 13: Detail of the local FEM loaded with boundary displacements + rotations from global FEM

4.2 Stress Intensity Factor (SIF)

SIF also known as K , describes the stress state surrounding a crack tip [10][11]. SIF methodology belongs to Linear Elastic Fracture Mechanics (LEFM). K value is required for SHM prognosis: for the estimation of the TB residual life, and it is function of the applied stress, the crack size, and the geometry of the component, see equation (1).

$$K = \beta\sigma\sqrt{\pi a} \quad (1)$$

being:

- β : geometric factor function of the structure geometry and load conditions.
- σ : applied stress far from the crack.

- $2a$: crack length.

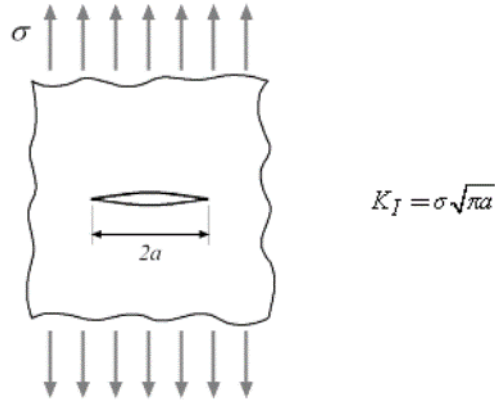


Figure 14: SIF for an infinite wide plate loaded in tension, $\beta = 1$

SIF values for numerous configurations are available in the literature [11][12][13][14]. Structural failure (unstable damage growth) at static load happens when SIF grows beyond fracture toughness of the material K_C .

4.2.1 SIF calculation within MSC.Nastran

Within MSC.Nastran [3][4] several solutions are available for SIF calculation, as:

- **Crack tip elements (CTE):** CRAC2D (plate type, see topology in Figure 15) and CRAC3D (solid type) elements according to MSC.Nastran. SIF is directly given as a result at the CTE.

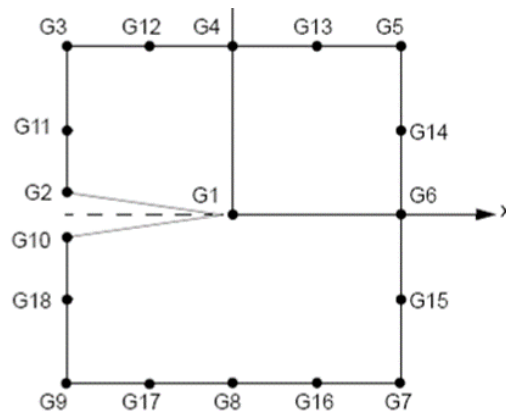


Figure 15: CTE CRAC2D topology

- **Virtual Crack Closure Technique (VCCT):** calculates the Strain Energy Release Rate (SERR), commonly referred as G . It is the increment in the elastic strain energy ΔU because of an increment in the crack area ΔA [15][16][17][18][19], and it may have 3 components: mode *I* due to opening tension, mode *II* due to in-plane shear, and mode *III* due to tearing shear. In Figure 16 a scheme of the required crack tip forces and displacements near crack tip in a 2D FEM is shown, and in equations (2) and (3)

the formulae for G_I and G_{II} calculations [18] are shown.

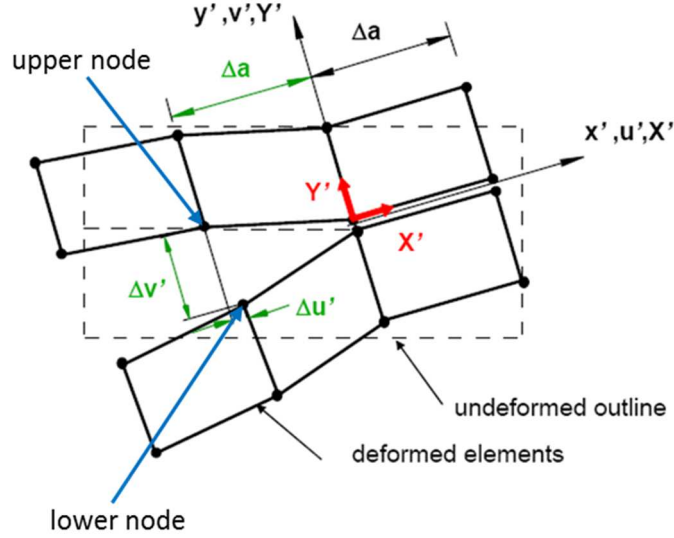


Figure 16: FEM scheme near crack tip for VCCT calculations

$$G_I = \frac{\Delta U_I}{\Delta A} = \frac{\left(\frac{1}{2} F_Y' \Delta v'\right)}{\Delta A} = \frac{1}{2} \frac{F_Y' (v'_{upper} - v'_{lower})}{\Delta a \times t} \quad (2)$$

$$G_{II} = \frac{\Delta U_{II}}{\Delta A} = \frac{\left(\frac{1}{2} F_X' \Delta u'\right)}{\Delta A} = \frac{1}{2} \frac{F_X' (u'_{upper} - u'_{lower})}{\Delta a \times t} \quad (3)$$

being:

- ΔU_I and ΔU_{II} are the strain energy increments released in modes I or II respectively, due to the growth of the crack Area (or delamination Area) in ΔA .
- ΔA : Crack area increase, that it is equal to Δa (mesh size) $\times t$ (thickness), see Figure 16.
- F_X' and F_Y' are the forces at the crack tip (in Figure 16 these forces are represented as red colour arrows).
- u' are the displacements of the closest nodes to the crack tip (upper and lower nodes as represented in Figure 16), along local coordinate axis X' .
- v' are the displacements of the closest nodes to the crack tip, the first nodes that can actually separate from each other, along local coordinate axis Y' .

Based in G_I value the SIF in mode I , the mode relevant one for ASTAYNAX TB, can be derived:

$$K_I = \sqrt{G_I E} \quad (4)$$

Both solutions, CTE and VCCT, were compared with published results in the literature and showed to provide accurate SIF results. VCCT was finally selected because FEM mesh is more easily parameterized.

3.3 Comparison of global and local FEMs

An initial comparison was performed between the stress contours at the global FEM (in the part of the structure covered by the local FEM), and local FEM itself (un-cracked configuration), see Figure 17. Both FEMs provide coherent stress results. Maximum stress is similar (3% difference), also shape of the stress plot is similar.

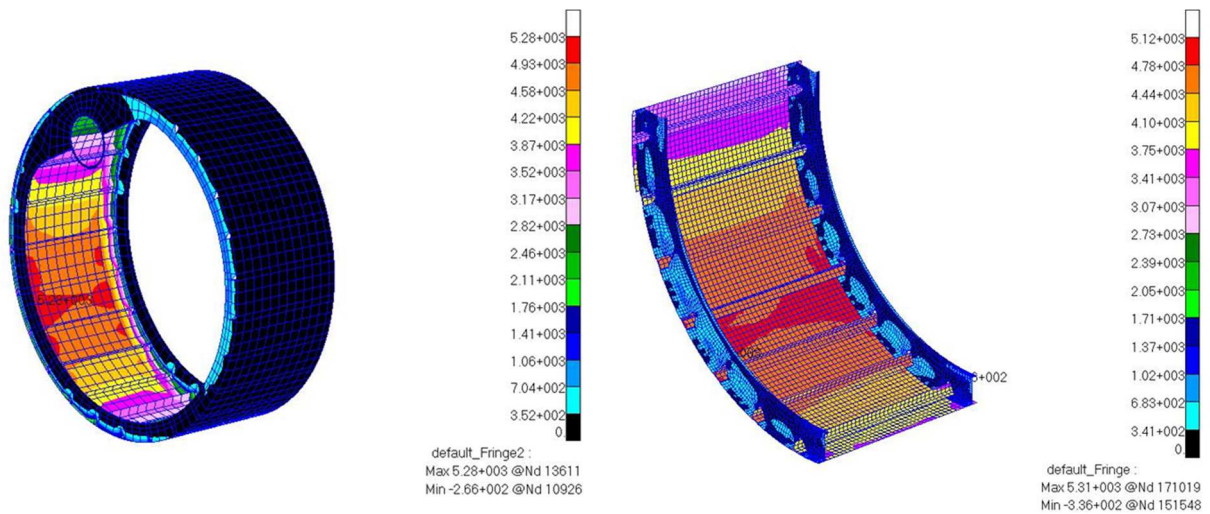


Figure 17: Contours of Maximum principal stress (Pa), for the Load case $F_Y = 1$ N

5 FATIGUE TESTS SIMULATION

The crack growth fatigue process for a metallic material depends among others on two factors:

- The applied increment in SIF (ΔK) across the fatigue loading.
- The applied force ratio R ($\sigma_{\min}/\sigma_{\max}$).

The information is recovered in a family of fatigue crack growth curves found by tests, that represents, for a specific material including its specific thermal heating or cold working, the crack growth rate da/dN (N is the number of applied fatigue cycles) versus the applied increment in SIF ΔK . For each R value a different curve is generated. These curves usually have 3 regions [20][21], as shown in Figure 18:

- Region 1: Threshold and near-threshold region: There is a minimum value of ΔK to actually have crack growth, this minimum value is called the threshold value $\Delta K_{\text{threshold}}$.
- Region 2: Crack growth rate da/dN is basically a linear function of the applied increment in SIF ΔK .
- Region 3: Toughness Asymptote region: when the applied increment in SIF ΔK is high enough (ΔK_{max}), crack growth becomes unstable, in other words da/dN becomes almost infinite.

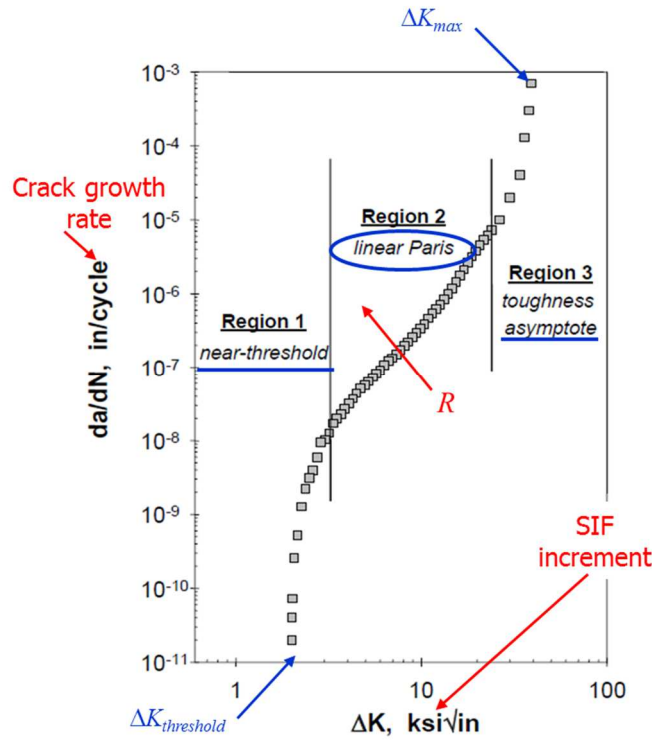


Figure 18: Typical fatigue crack growth curve for metallics [20]

The ASTYANAX local FEM has been used to simulate the TB fatigue test, providing support to determine:

- Size of the initial notch, so that the applied SIF increment ΔK at the fatigue tests is at region 2, so the crack growth process is not too slow (region 1), or too fast or even unstable (region 3).
- Critical crack length: this is an important parameter for the tests. This is derived when the applied ΔK is equal to the material ΔK_{max} (asymptote of region 3).

5.1 Strain sensitivity to crack length

This is a crucial verification to properly design the SHM diagnostic system: it has to be verified that the strains read by sensors are sensitive to variations of crack size. The tested TB will have bonded FBGS measuring longitudinal strain at the stringers. By using the local FEM, the strain ($\mu\epsilon$) measured by the SHM optical sensors were simulated considering a crack at the central rivet of stringer 8, transversal to stringer axis, and different crack lengths: from 5 to 100 mm, each 5 mm.

In Figure 19 the position of 10 of the sensors that will be used in the tests is shown: sensors 1 to 5 in the stringer 8 just above the skin crack, and sensors 6 to 10 in the stringer 7. In Figure 20, and in Figure 21 curves “strain versus crack length” measured at the 10 sensors are shown.

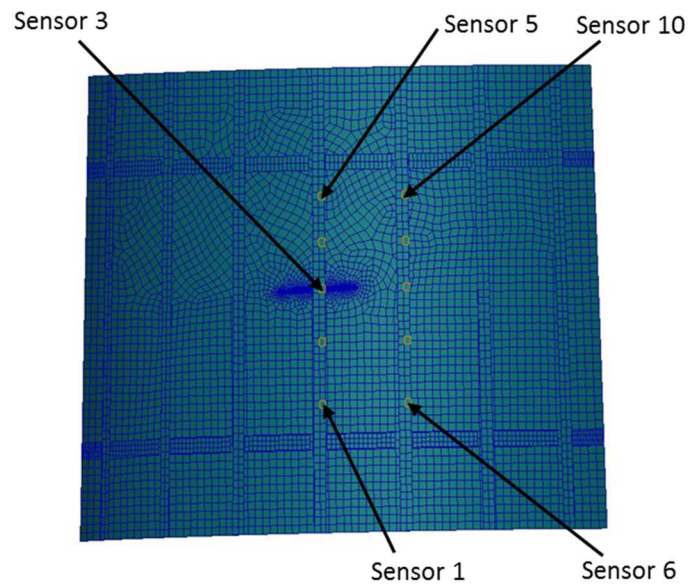


Figure 19: Positions of sensors 1 to 10 in stringers 8 (above the crack), and 7

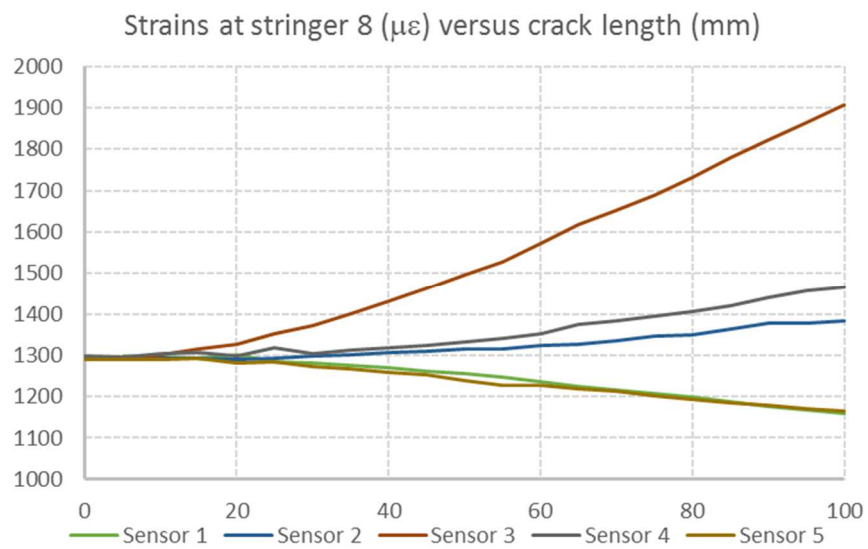


Figure 20: Strains at stringer 8 (stringer above the crack) versus crack length

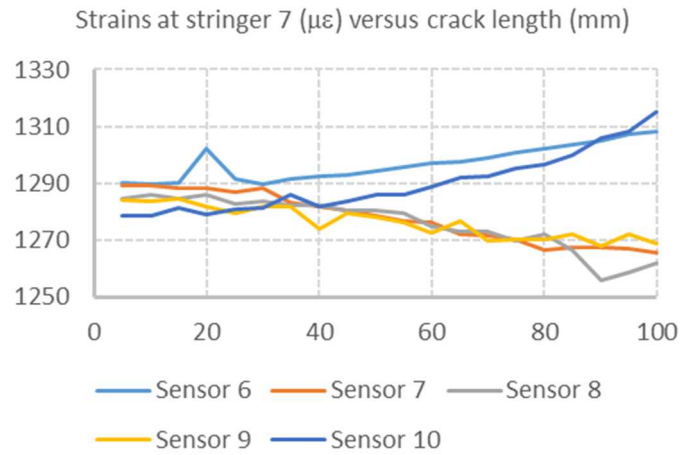


Figure 21: Strains at stringer 7 versus crack length

In Figure 22, strain contours (strain along stringer direction) are shown for the un-cracked TB FEM, and for 3 cracked versions: 10 mm, 50 mm, and 100 mm. The cracks are in all cases at the skin, at the central rivet hole of stringer 8, and transversal to stringer axis. As it can be seen, maximum strain value increases the higher the crack length is.

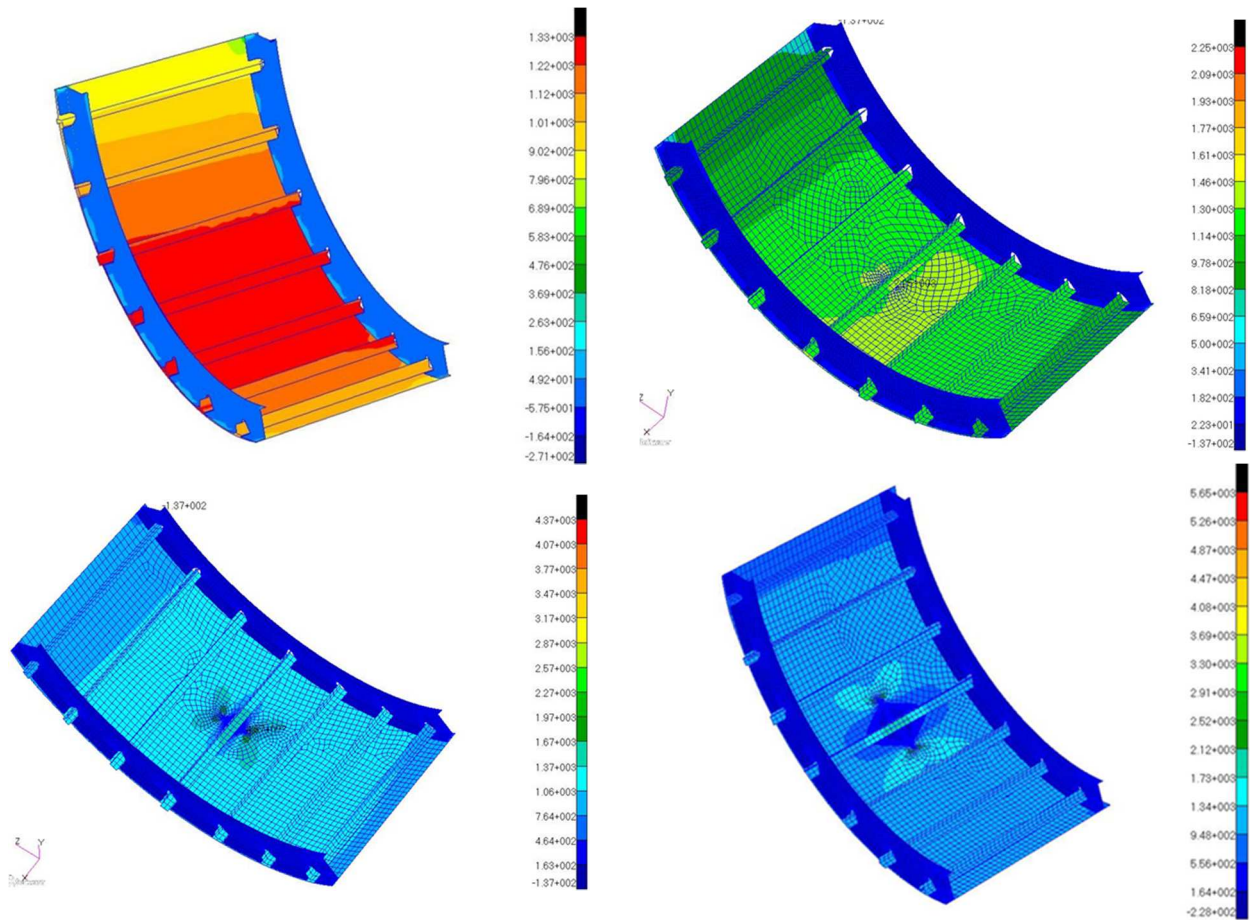


Figure 22: Strains ($\mu\epsilon$) along stringer direction, for the maximum applied load during TB Fatigue Tests (Up-left: un-cracked. Up-right: 10 mm crack. Down-left: 50 mm crack. Down-right: 100 mm crack)

In Figure 23, a detail plot of $\Delta\epsilon^*$, the strain increment (strain along stringer direction) for the 100 mm cracked FEM referenced from the strain level at the un-cracked FEM is shown.

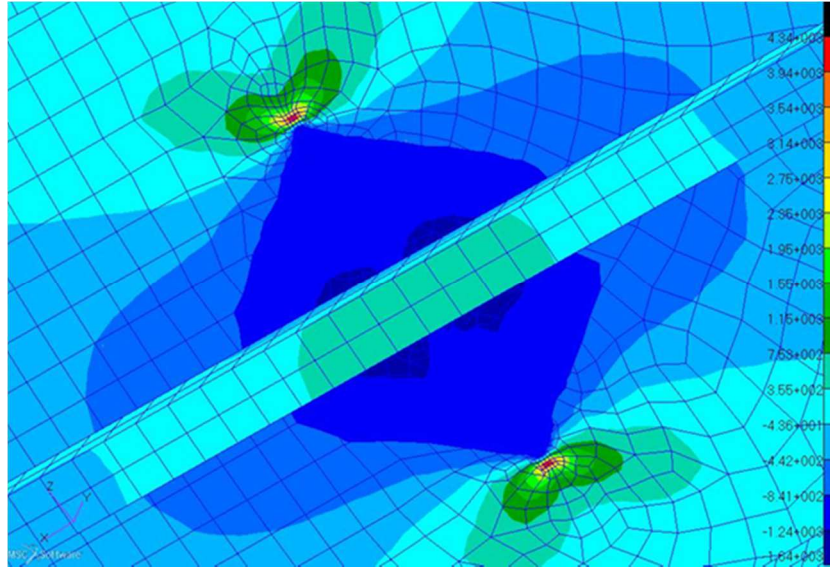


Figure 23: Plots of $\Delta\epsilon^*$: strain at 100 mm cracked FEM minus strain at un-cracked FEM ($\mu\epsilon$)

*: strain along stringer direction

FEM predictions indicate that the strain field and, therefore, the strain read by the SHM optical sensors, are in principle quite sensitive to variations of crack length. Therefore, the conclusion is that there is a high probability of accurate crack detection, location, and quantification. This will be confirmed during the TB Fatigue Tests.

6 SHM SYSTEM TRAINING DATABASE

The family of cracked local TB FEMs are used to generate the simulated experience required to train the ANN algorithms, the heart of the SHM system. As above referenced, the damage mode considered is a crack at the skin of the TB at a rivet hole (stringer-skin I/F), a quite common damage mode in this type of structures. The parameters used for local FEM generation are:

- Crack position: each rivet hole between 2nd and 3rd frame.
- Crack angle respect to the transversal stringer axis. For the moment, only angle = 0° (crack perpendicular to the stringer) has been considered. This is because in the Fatigue tests the initial notch will be perpendicular to the stringer, and it is expected that the crack keeps that angle when growing. For future developments, other angle values can be simulated.
- Crack length: 5 – 100 mm, each 5 mm.

The following results were found from local FEMs:

- Strain at the stringers elements (position of the optical sensors at the fatigue tests) along the longitudinal axis. These strains are required for the diagnostic algorithm

of the SHM system.

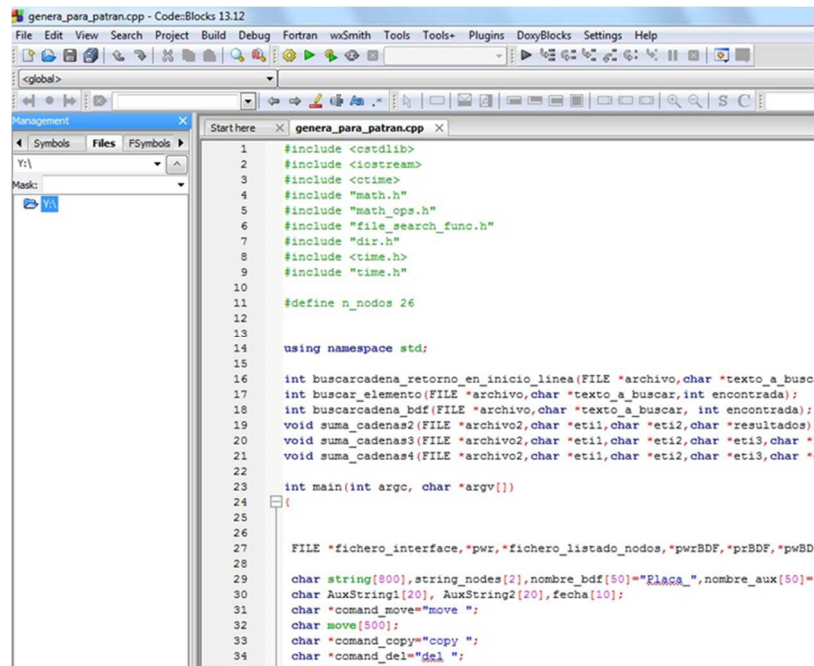
- Stress Intensity Factors (SIF) at left and right crack tips. These SIF values are required for the prognostic algorithm that estimates the TB residual life.

6.1 FEM Parameterization

It has been done by means of an executable program generated with C++ Language, using Code::Blocks compiler 13.12 [22]. The executable performs a quite complex operations sequence:

- Opens the Pre/post Patran.
- According to the selected crack parameters (defined within an automatic loop), it generates a Patran Command Language (PCL) file with the operations sequence required to generate the TB cracked skin according to the crack parameters.
- Run that PCL sequence inside Patran. The PCL makes Patran first to generate (and mesh) a flat cracked skin, and second to project it onto the real curved surface of the TB.
- Generates a Nastran input file (bdf format) of the cracked curved skin.
- Opens a new Patran session importing the cracked curved skin mesh, and joins it a file containing stringers elements, frames elements, and rivets (CFAST connectors).
- Applies boundary conditions for the local FEM, based in global FEM results (displacements + rotations).
- Generates a complete Nastran file of the whole local FEM. Runs the Nastran input file.
- Reads the Nastran results file (f06 format): strain at the stringers, and displacements near crack tip, and GPFORCES (nodal forces) at crack tips. With these values, and using MVCCT formulae, the executable calculates SIFs for both left and right crack tips.
- Writes SIF and strain results in the SHM training database.

In Figure 24 a General view of Code::Blocks compiler and the used C++ source code is shown, while in Figure 25 a partial view of a PCL file (it is a text format file) is shown.

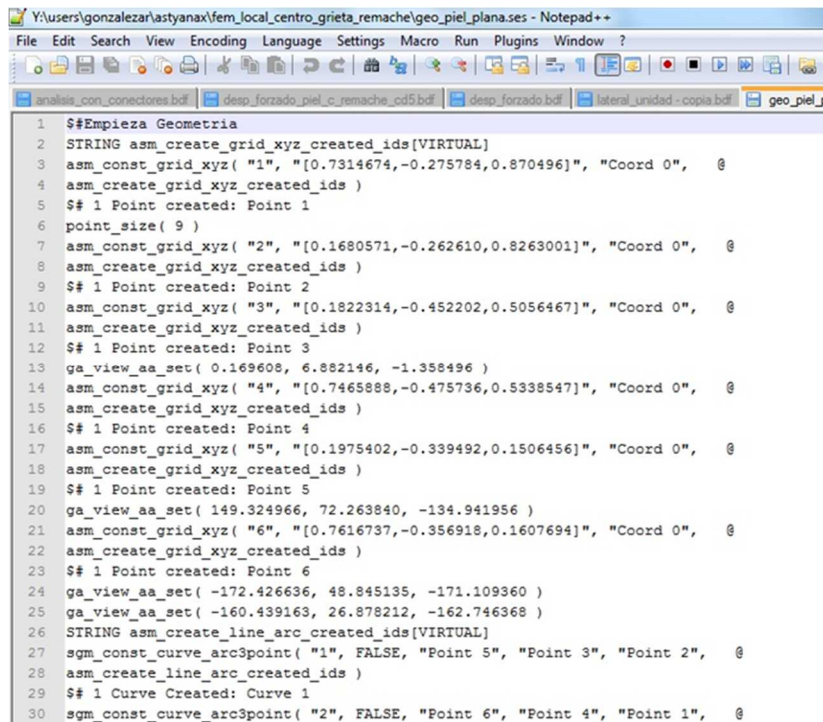


```

1  #include <cstdlib>
2  #include <iostream>
3  #include <ctime>
4  #include "math.h"
5  #include "math_ops.h"
6  #include "file_search_func.h"
7  #include "dir.h"
8  #include <time.h>
9  #include "time.h"
10
11 #define n_nodos 26
12
13
14 using namespace std;
15
16 int buscarcadena_retorno_en_inicio_linea(FILE *archivo, char *texto_a_busca
17 int buscar_elemento(FILE *archivo, char *texto_a_buscar, int encontrada);
18 int buscarcadena_bdf(FILE *archivo, char *texto_a_buscar, int encontrada);
19 void suma_cadenas2(FILE *archivo2, char *et1, char *et2, char *resultados);
20 void suma_cadenas3(FILE *archivo2, char *et1, char *et2, char *et3, char *r
21 void suma_cadenas4(FILE *archivo2, char *et1, char *et2, char *et3, char *e
22
23 int main(int argc, char *argv[])
24 {
25
26
27     FILE *fichero_interface, *pwz, *fichero_listado_nodos, *pwzBDF, *pwBDF
28
29     char string[800], string_nodos[2], nombre_bdf[50]="Placa_", nombre_aux[50]="
30     char AuxString1[20], AuxString2[20], fecha[10];
31     char *command_move="move ";
32     char move[500];
33     char *command_copy="copy ";
34     char *command_del="del ";

```

Figure 24: General view of Code::Blocks compiler and the C++ source code



```

1  $#Empieza Geometria
2  STRING asm_create_grid_xyz_created_ids[VIRTUAL]
3  asm_const_grid_xyz( "1", "[0.7314674,-0.275784,0.870496]", "Coord 0", @
4  asm_create_grid_xyz_created_ids )
5  $# 1 Point created: Point 1
6  point_size( 9 )
7  asm_const_grid_xyz( "2", "[0.1680571,-0.262610,0.8263001]", "Coord 0", @
8  asm_create_grid_xyz_created_ids )
9  $# 1 Point created: Point 2
10 asm_const_grid_xyz( "3", "[0.1822314,-0.452202,0.5056467]", "Coord 0", @
11 asm_create_grid_xyz_created_ids )
12 $# 1 Point created: Point 3
13 ga_view_aa_set( 0.169608, 6.882146, -1.358496 )
14 asm_const_grid_xyz( "4", "[0.7465888,-0.475736,0.5338547]", "Coord 0", @
15 asm_create_grid_xyz_created_ids )
16 $# 1 Point created: Point 4
17 asm_const_grid_xyz( "5", "[0.1975402,-0.339492,0.1506456]", "Coord 0", @
18 asm_create_grid_xyz_created_ids )
19 $# 1 Point created: Point 5
20 ga_view_aa_set( 149.324966, 72.263840, -134.941956 )
21 asm_const_grid_xyz( "6", "[0.7616737,-0.356918,0.1607694]", "Coord 0", @
22 asm_create_grid_xyz_created_ids )
23 $# 1 Point created: Point 6
24 ga_view_aa_set( -172.426636, 48.845135, -171.109360 )
25 ga_view_aa_set( -160.439163, 26.878212, -162.746368 )
26 STRING asm_create_line_arc_created_ids[VIRTUAL]
27 sgm_const_curve_arc3point( "1", FALSE, "Point 5", "Point 3", "Point 2", @
28 asm_create_line_arc_created_ids )
29 $# 1 Curve Created: Curve 1
30 sgm_const_curve_arc3point( "2", FALSE, "Point 6", "Point 4", "Point 1", @

```

Figure 25: Partial view of the PCL code

In Figure 26, and in Figure 27, two different intermediate steps of the parametric local FEM generation are shown.

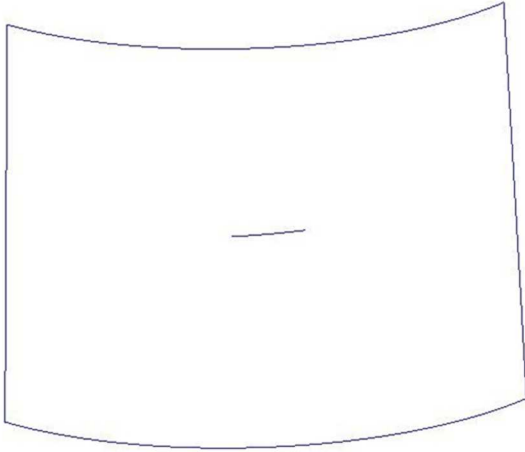


Figure 26: Intermediate step of the parametric local FEM generation: cracked surface

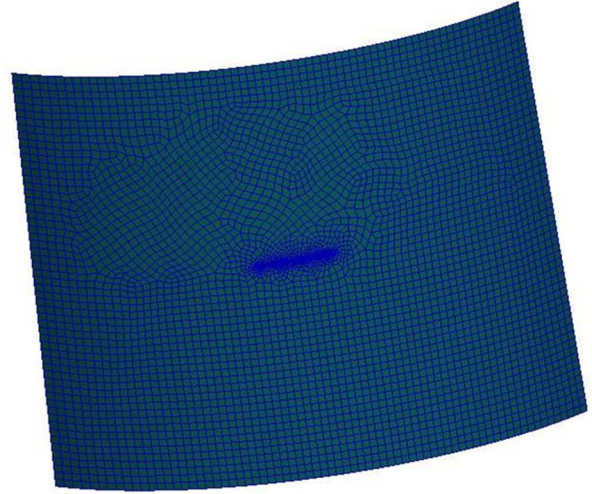


Figure 27: Intermediate step of the parametric FEM generation: cracked skin mesh

6.2 SHM training database

In Table 1 the structure of the SHM training database is shown. Each row of the database corresponds to a different crack configuration (different crack parameters), and at each row there are 159 columns for case identification (columns 1 to 7), SIF results (columns 8 and 9), and strain results (columns 10 to 159).

Column	Content
1	Stringer number from which crack originates
2	Rivet number from which crack originates
3 - 5	X, Y, and Z position of the rivet (m)
6	Crack length (m)
7	Crack angle respect to stringer direction (°)
8	K_I (SIF) at the left tip of the crack ($\text{MPa m}^{1/2}$)
9	K_I (SIF) at the right tip of the crack ($\text{MPa m}^{1/2}$)
10 - 159	Strain in longitudinal direction ($\mu\epsilon$) at stringer elements, in the same positions of FBGS used in the TB fatigue tests

Table 1: Structure of the SHM “training” database

7 CONCLUSIONS

ASTYANAX is a Research project promoted by the European Defence Agency (EDA) focused on the development of reliable methodologies for Structural Health Monitoring (SHM) of rotary and fixed-wing platforms. ASTYANAX focuses in 2 types of damages: local

plastifications caused by hard landings, and cracks originating in rivet holes that grow during the operational life of the vehicle.

Demonstrations are made to a full scale metallic helicopter: the Mi 8/17 Hip. Two kind of tests are performed, the first one are drop tests from increasing height made to the whole helicopter with the aim of identifying the onset of local plastifications. The other are fatigue tests of the helicopter tail boom (TB), that will have an initial notch, and its progression will be monitored across the tests. The TB will be equipped with a sensor network.

The readings of the sensors (strain for instance) will be the inputs of an SHM system designed within ASTYANAX with diagnostic and prognostic capabilities. This SHM system has been designed by using ANN algorithms.

In the paper the FEA approach used for the TB and the fatigue crack process has been explained in detail. The FEA has a double aim: first to simulate TB fatigue tests and to determine relevant test features such as an adequate size of the initial notch, the critical crack length, the crack growth rate, and the sensitivity of sensor strain readings to crack length.

The second FEA aim is to generate the training database of the SHM system. This has been done by using parametric TB FEM versions considering multiple crack configurations. ANN algorithms, the heart of the SHM system, requires a high number of cases in the order of thousands or more, for a proper training.

FEA accuracy is, therefore, very important for an adequate design of the SHM systems. The strategies followed for FEM parameterization and automation, and for derivation of strain and SIF results are explained in this paper. The final validation of the FEA, and the diagnostic and prognostic capabilities of the SHM system, will be made with the sensor readings during the TB fatigue tests.

8 REFERENCES

- [1] C. Sbarufatti, A. Manes, and M. Giglio, "HECTOR: one more step toward the embedded Structural Health Monitoring system", CEAS 2011 International Aerospace Conference, Venice (2011).
- [2] G. Vallone, C. Sbarufatti, A. Manes, and M. Giglio, "Artificial Neural Networks for Structural Health Monitoring of Helicopter Harsh Landings", Applied Mechanics and Materials Vol. 390, 192-197 (2013).
- [3] "MSC Nastran 2012, Quick Reference Guide", MSC Software.
- [4] "MSC Nastran 2012, Linear Static Analysis - User's Guide", MSC Software.
- [5] "MSC Nastran 2012, SuperElement User's Guide", MSC Software.
- [6] "MSC Patran 2012, User's Guide", MSC Software.
- [7] "MSC Patran 2012, Reference Manual Part 3: Finite Element Modelling", MSC Software.
- [8] "MSC Patran 2012, Interface to MSC.NASTRAN, Preference Guide. Volume 1: Structural Analysis", MSC Software.
- [9] G. Ahlbert, "Method Evaluation of Global-Local Finite Element Analysis". Diss. Linköping, 2012.
- [10] T. L. Anderson, "Fracture mechanics: Fundamentals and Applications," CRC Press (2005).

- [11] H. Tada, P. C. Paris, G. R. Irwin, “The stress analysis of cracks handbook”, ASME Press (2000).
- [12] S. Al. Laham, “Stress Intensity Factor and Limit Load Handbook”, British Energy Generation Ltd, 1998.
- [13] T. Fett, “Stress intensity factors and weight functions for special crack problems”, Institut für Materialforschung, Forschungszentrum Karlsruhe GmbH, Karlsruhe (1998).
- [14] “NASGRO - Fracture Mechanics and Fatigue Crack Growth Analysis Software”, version 7 (2012), Southwest Research Institute.
- [15] E. F. Rybicki, M. F. Kanniken, “A Finite Element Calculation of Stress Intensity Factors by a Modified Crack Closure Integral”, Engineering Fracture Mechanics, Volume 9, issue 4 931-938 (1977).
- [16] D. Xie, S. B. Biggers Jr., “Progressive crack growth analysis using interface element based on the virtual crack closure technique”, Finite Elements in Analysis and Design 42 977 – 984 (2006).
- [17] A. C. Orifici, R. Krueger, ”Benchmark assessment of automated delamination propagation capabilities in finite element codes for static loading”, Finite Elements in Analysis and Design 54 28–36 (2012).
- [18] R. Krueger, “Computational Fracture Mechanics for Composites - State of the Art and Challenges”, CAA/FAA Workshop on Adhesive Bonding, Gatwick, UK, October 2004.
- [19] A. Leski, “Implementation of the Virtual Crack Closure Technique in engineering FE calculations”, Finite Elements in Analysis and Design 43 261 – 268 (2007).
- [20] R. G. Forman, V. Shivakumar, J. W. Cardinal, L. C. Williams and P. C. McKeighan, “Fatigue Crack growth database for Damage Tolerance Analysis”, FAA document DOT/FAA/AR-05/15.
- [21] R. C. Rice, J. L. Jackson, J. Bakuckas, and S. Thompson, “Metallic Materials Properties Development and Standardization (MMPDS)”, FAA document DOT/FAA/AR-MMPDS-01.
- [22] CodeBlocks Manual, HighTec EDV-Systeme GmbH (2010).

ACKNOWLEDGMENTS

This work has been developed based on the results from ASTYANAX project (Aircraft fuSelage crack monitoring sYstem And progNosis through on-boArd eXpert sensor network), a Cat.-B project coordinated by the European Defense Agency (EDA) and involving three nations: Italy (Politecnico di Milano, AleniaAermacchi, AgustaWestland), Poland (Instytut Techniczny Wojsk Lotniczych - AFIT, Military Aviation Works No. 1, AGH University of Science and Technology) and Spain (Instituto Nacional de Técnica Aeroespacial - INTA).